International Journal of Engineering Research & Technology (IJERT)
ISSN: 2278-0181
Vol. 3 Issue 11, November-2014

Magnetohydrodynamic Free Convection in a Square Cavity with Semicircular Heated Block

Abdul Halim Bhuiyan[1]
Department of Mathematics
Bangladesh University of Engineering and Technology
Dhaka-1000, Bangladesh

Rafiqul Islam[2]
Department of Mathematics
Khulna University of Engineering & Technology
Khulna-9203, Bangladesh

M. A. Alim[3]
Department of Mathematics
Bangladesh University of Engineering and Technology
Dhaka-1000, Bangladesh

***Abstract*—In this paper, the effect of magnetic field in a square cavity with semicircular heated block are studied numerically. The governing differential equations are solved by using finite element method (weighted-residual method). Here the side walls of the cavity are assumed to be adiabatic, the top wall is kept at cold and bottom wall is heated. Also all the wall are assumed to be no-slip condition. The study is performed for different Rayleigh and Hartmann numbers at Pr=0.71. The results are illustrated with the streamlines, isotherms, velocity and temperature fields as well as local Nusselt number.**

Keywords—Finite element method; Hartmann number; semicircular heated block; square cavity.

I. INTRODUCTION

Convection heat transfer has an important role in the practice application in leady life. Application of natural convection heat transfer is very much common in engineering field such as solar collector, heat exchanger, building heating and cooling etc. Most of the cavities frequently used in industries are cylindrical, rectangular, square, trapezoidal and triangular etc. Square cavities have received a considerable attention for its application in various fields. Many numerical investigations on free convection in different types of cavities have been investigated in the recent year. Natural convection heat transfer in a square cavity with a heated plate built-in vertically and horizontally was investigated by Oztop and Dagtekin (2004). They addressed the effect of the position and aspect ratio of heated plate on heat transfer and fluid flow and it was found that mean Nusselt numbers at both vertical and horizontal location increased as Rayleigh number increased. Basak and Roy (2005) investigated the natural convection flows in a square cavity with non-uniformly heated walls. A penalty finite element analysis with biquadratic rectangular elements is performed to investigate the influence of uniform and non-uniform heating of walls on natural convection flows in a square cavity. In this investigation one vertical wall and the bottom wall are uniformly and non-uniformly heated while the other vertical wall is maintained at constant cold temperatures and the top wall is well insulated. In case of uniform heating, the heat transfer rate is very high at the right edge of the bottom wall and almost uniform at the rest part of the bottom wall as well as at the hot vertical wall. In contrast, for the case of non-uniform heating the heat transfer rate is minimum at the edges of the heated walls and the heat transfer rate reaches its maximum value at the centre of both the heated walls.

Basak et al. (2006) investigated the effects of thermal boundary conditions on natural convection flows within a square cavity. Mehmet and Elif (2006) studied the natural convection flow under a magnetic field in an inclined rectangular enclosure heated and cooled on adjacent walls. It was observed that the orientation and the aspect ratio of the enclosure and the strength and direction of the magnetic field have significant effects on the flow and temperature fields. Saha et al. (2007) studied the natural convection flow in a square tilt open cavity where the finite element method is used as the method of solution. They found that the heat transfer increases with the increase of Rayleigh numbers. Öztop and Al-Salem (2012) numerically investigated effects of joule heating on MHD natural convection in non-isothermally heated enclosure. They observed that positive stream functions are decreased with increasing of Hartmann number and thermal boundary layer becomes larger.

Jani et al. (2013) investigated numerically Magnetohydrodynamic free convection in a square cavity heated from below and cooled from other walls. They used finite volume method and showed that the transfer mechanisms, temperature distribution and the flow characteristics inside the cavity depended strongly upon both the strength of the magnetic field and the Rayleigh number. Also they found that using the longitudinal magnetic field results in a force (Lorentz force) opposite to the flow direction that tends to decrease the flow velocity. Moreover they observed that, for low Rayleigh numbers, by increase in the Hartman number, free convection is suppressed and heat transfer occurs through conduction mainly. From the above literatures, the aim of present investigation is to investigate the effect of magnetic field in a square cavity with semicircular heated block.

II. MODEL AND MATHEMATICAL FORMULATION

The Fig. 1 shows a schematic diagram and the coordinates of a two-dimensional square cavity, where the bottom wall and semicircular block are maintained at a hot temperature T_h and the side walls maintained adiabatic whereas top wall is cold temperature T_c. The fluid is permeated by a uniform magnetic field B_0 which is applied normal to the direction of the flow and the gravitational force (g) acts in the vertically downward direction.

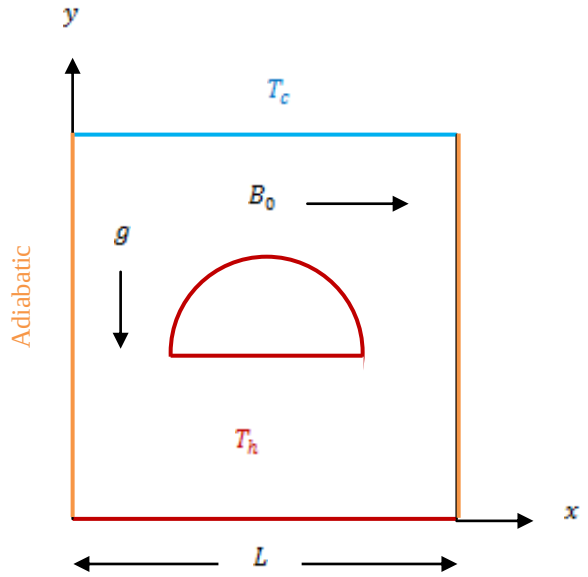

Fig. 1. The flow configuration and coordinate system

The fluid properties, including the electrical conductivity, are considered to be constant, except for the density, so that the Boussinesq approximation is used. Neglecting the radiation mode of the heat transfer and Joule heating, the governing equations for mass, momentum and energy of a steady two-dimensional natural convection flow in a cavity are as follows:

$$\frac{\partial u}{\partial x}+\frac{\partial v}{\partial y}=0 \tag{1}$$

$$\rho\left(u\frac{\partial u}{\partial x}+v\frac{\partial u}{\partial y}\right)=-\frac{\partial p}{\partial x}+\mu\left(\frac{\partial^2 u}{\partial x^2}+\frac{\partial^2 u}{\partial y^2}\right) \tag{2}$$

$$\rho\left(u\frac{\partial v}{\partial x}+v\frac{\partial v}{\partial y}\right)=-\frac{\partial p}{\partial y}+\mu\left(\frac{\partial^2 v}{\partial x^2}+\frac{\partial^2 v}{\partial y^2}\right)+\rho g\beta(T-T_c)-\sigma B_0{}^2 v \tag{3}$$

$$u\frac{\partial T}{\partial x}+v\frac{\partial T}{\partial y}=\alpha\left(\frac{\partial^2 T}{\partial x^2}+\frac{\partial^2 T}{\partial y^2}\right) \tag{4}$$

The governing equations are nondimensionalized using the following dimensionless variables:

$$X=\frac{x}{L},\quad Y=\frac{y}{L},\quad U=\frac{uL}{\alpha},\quad V=\frac{vL}{\alpha},$$

$$P=\frac{pL^2}{\rho\alpha^2},\theta=\frac{T-T_c}{T_h-T_c},\quad \sigma=\frac{\rho^2\alpha}{L^2},\quad \alpha=\frac{k}{\rho C_p}$$

Introducing the above dimensionless variables, the following dimensionless forms of the governing equations are obtained as follows:

$$\frac{\partial U}{\partial X}+\frac{\partial V}{\partial Y}=0 \tag{5}$$

$$U\frac{\partial U}{\partial X}+V\frac{\partial U}{\partial Y}=-\frac{\partial P}{\partial X}+\Pr\left(\frac{\partial^2 U}{\partial X^2}+\frac{\partial^2 U}{\partial Y^2}\right) \tag{6}$$

$$U\frac{\partial V}{\partial X}+V\frac{\partial V}{\partial Y}=-\frac{\partial P}{\partial Y}+\Pr\left(\frac{\partial^2 V}{\partial X^2}+\frac{\partial^2 V}{\partial Y^2}\right)+\frac{Ra}{\Pr}\theta-Ha^2\Pr V \tag{7}$$

$$U\frac{\partial \theta}{\partial X}+V\frac{\partial \theta}{\partial Y}=\frac{\partial^2 \theta}{\partial X^2}+\frac{\partial^2 \theta}{\partial Y^2} \tag{8}$$

Here Pr is the Prandtl number, *Ra* is the Rayleigh number and *Ha* is the Hartmann number, which are defined as:

$$\Pr=\frac{\nu}{\alpha},\ Ha^2=\frac{\sigma B_0{}^2 L^2}{\mu},\ Ra=\frac{g\beta L^3(T_h-T_c)\Pr}{\nu^2}$$

The corresponding boundary conditions then take the following form:

$$U=V=0,\theta=1(\text{on the bottom wall and semicircular block})$$

$$U=V=0,\theta=0(\text{on the top wall})$$

$$U=V=0,\frac{\partial\theta}{\partial N}=0(\text{at side walls})$$

$$P=0\begin{pmatrix}\text{fluid pressure, at the inside and on the}\\ \text{wall of the enclosure}\end{pmatrix}$$

III. NUMERICAL PROCEDURE

The Galerkin weighted residual method of finite element formulation is used to solve the dimensionless governing equations with the boundary conditions. This technique is well described by (1993). In this method, the solution domain is discretized into finite element meshes and then the nonlinear governing equations are transferred into a system of integral equations by applying the Galerkin weighted residual method. Gauss quadrature method is used to perform the integration involved in each term of these equations. The nonlinear algebraic equations which are obtained are modified by imposition of boundary conditions and Newton's method is used to transform these modified equations into linear algebraic equations, and then these linear equations are solved by applying the triangular factorization method.

IV. CODE VALIDATION

Validation of the code was done by comparing streamlines and isotherms with results shown in Fig. 2(a) and Fig. 2(b) by Jani et al. (2013). As seen from these figures the obtained results show good agreement.

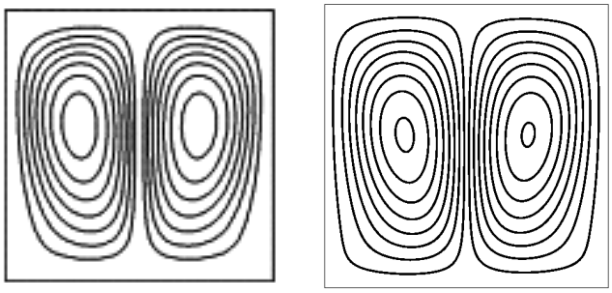

Jani et al. (2013) Present work

Fig. 2(a). Obtained results for Streamlines while *Ha=0*, Pr=0.7 and *Ra*=10^5

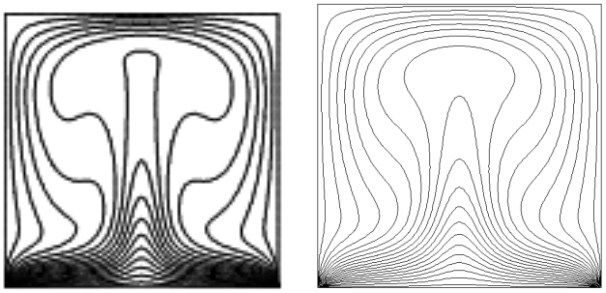

Jani et al. (2013) Present work

Fig. 2(b). Obtained results for Isotherms while *Ha=0*, Pr=0.7 and *Ra*=10^5

V. RESULTS AND DISCUSSION

In this section, results have been obtained for the Rayleigh number ranging from 10^4 to 10^6 and the Hartman number varying from 0 to 100 with fixed Prandtl number Pr=0.71. The results are presented in terms of streamlines and isotherms inside the cavity, the vertical velocity component, dimensionless temperature and the local Nusselt number along the hot bottom wall.

Streamlines and isotherms for Ha = 0 (no magnetic field) are presented in Fig. 3 and Fig. 4 respectively to understand the effects of Rayleigh number on flow field and temperature distribution. At Ra = 10000 and in the absence of the magnetic field (Ha = 0) two cells are formed with two elliptic-shaped eyes topside of the semicircular heated block of the cavity shown in Fig. 3(a). At Ra = 100000 almost same result as Fig. 3(a) but flow strength increases shown in Fig. 3(b). For higher Rayleigh numbers four elliptic-shaped eyes are formed inside the cavity and also flow strength increases are shown in Fig. 3(c) and Fig. 3(d). Stream function has symmetrical value about the vertical central line as the semicircular heated block is symmetrical. Conduction dominant heat transfer is observed from the isotherms in Fig. 4(a) and Fig. 4(b) at Ra = 10000 and Ra = 100000. With increase in Rayleigh number, isotherms are concentrates near the top wall and isotherms lines are more bending which means increasing heat transfer through convection. Formation of thermal boundary layers can be found and increases from the isotherms for Ra = 500000 and Ra= 1000000 at Ha = 0 are shown in Fig. 4(c) and Fig. 4(d). Streamlines and isotherms for Ra = 10^5 are presented in Fig. 5 and Fig. 6 respectively to understand the effects of effects of Hartmann number on the flow and temperature fields. From the streamlines it is found that with increasing the Hartman number (increasing the strength of the magnetic field) the eyes of vortices slightly changes and decrease in the flow velocity and numbers of mainstream flows are increased with increasing Hartman number shown in Fig. 5(a-d). From the isotherms it is observed that with increase in Hartman number, free convection is suppressed and heat transfer occurs mainly through conduction. Slightly less bend of the isotherms lines is observed as the Hartmann number increases shown in Fig. 6(a-d). The local Nusselt number along the bottom wall for different Rayleigh number with Pr=0.71 and Ha=0 of the cavity are shown in Fig. 7(a). Minimum and maximum shape curves are obtained here. For X<0.2 maximum shape curves are found and for X>0.2 minimum shape curves are found and absolute value of local Nusselt number (that is heat transfer rate) is increased from the increasing of Rayleigh numbers. The local Nusselt number along the bottom wall for different Hartmann number with Pr=0.71 and Ra=10^5 of the cavity are shown in Fig. 7(b). Minimum and maximum shape curves are also obtained here. Absolute value of local Nusselt number is decreased from the increasing of Hartmann numbers. For X=0.2 the local Nusselt number has identical value zero for different Hartmann numbers and Rayleigh numbers. Variations of the vertical velocity component along the bottom wall for different Rayleigh number with Pr=0.71 and Ha=0 of the cavity are shown in Fig. 8(a). It can be seen from the Figure that the absolute value of maximum and minimum value of velocity increases with increasing the Rayleigh number (increasing the buoyant force). The curves are symmetrical parabolic shaped as the semicircular heated block is symmetrical. For lower Rayleigh number value of velocity has smaller changed but for higher Rayleigh number value of velocity has larger changed. Variations of the vertical velocity component along the bottom wall for different Hartmann number with Pr=0.71 and Ra=10^5 of the cavity are shown in Fig. 8(b). From the Figure it can be observed that the curves are symmetric about the line X=0.2 because of symmetrical semicircular heated block. The absolute value of maximum and minimum value of velocity decreases with increasing the Hartmann number. Fig. 9(a) presents the temperature profiles along the bottom wall for different Rayleigh number with Pr=0.71 and Ha=0. As seen from the Figure, temperature value is decreased from the increasing of Rayleigh numbers. Parabolic shape temperature profile is obtained due to symmetric shape of the semicircular heated block. For lower Rayleigh number temperature value has less significant changed but for higher Rayleigh number temperature value has more significant. Fig. 9(b) presents the temperature profiles along the bottom wall for different Hartmann number with Pr=0.71 and Ra=10^5. As seen from the Figure, temperature value is increased from the increasing of Hartmann numbers. Maximum shape temperature profile which symmetrical about X=0.2 is obtained due to symmetric shape of the semicircular heated block and the maximum point moves towards to top with decreasing of Hartmann number. For higher Hartmann number temperature value has tiny changed because for lower Rayleigh number conduction is dominant.

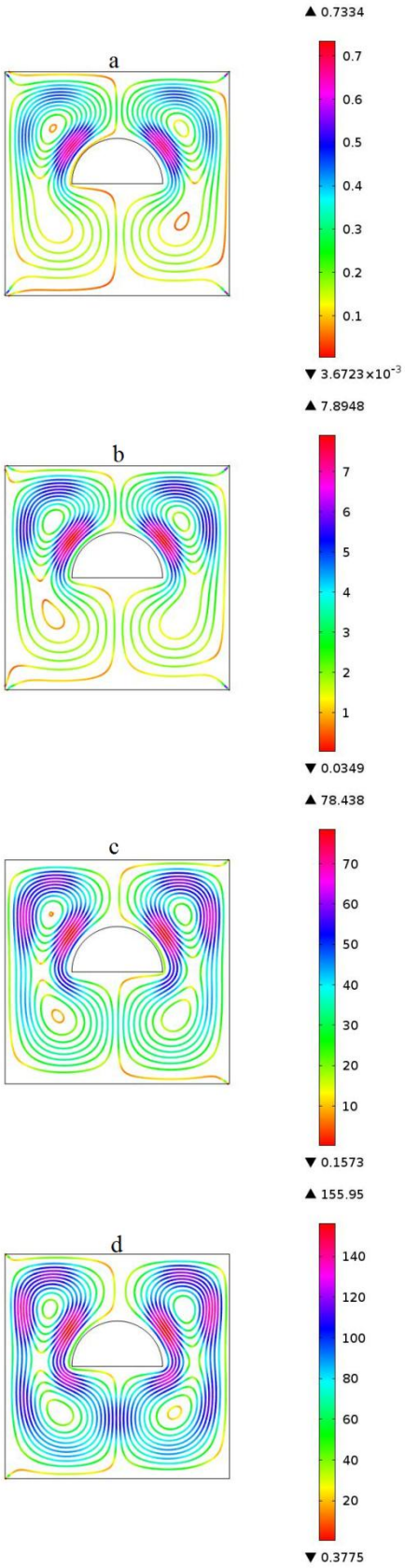

Fig. 3. Streamlines for (a) Ra=10000; (b) Ra=100000; (c) Ra=500000 (d) Ra=1000000 while *Ha*=0 and Pr=0.71.

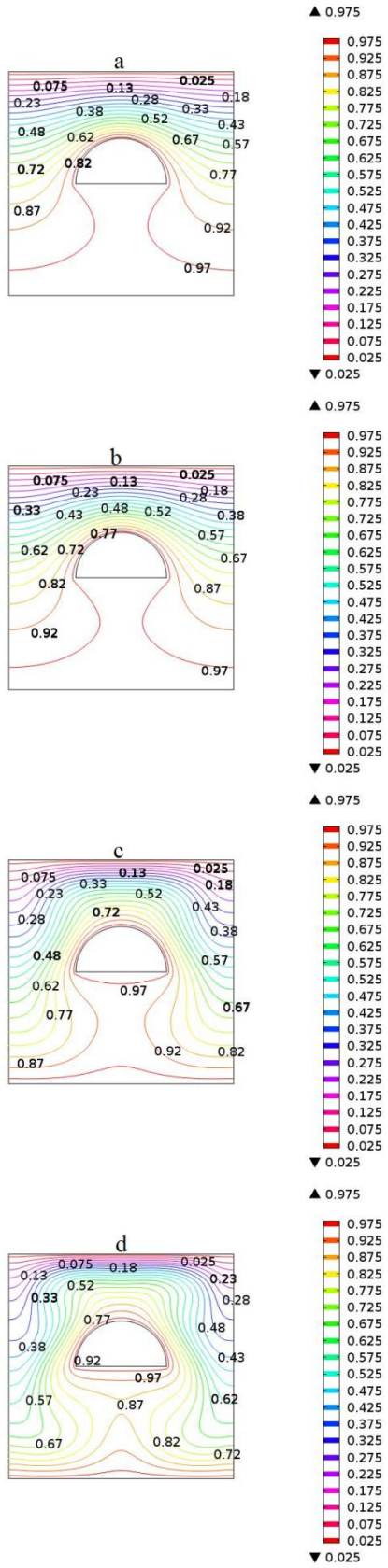

Fig. 4. Isotherms for (a) Ra=10000; (b) Ra=100000; (c) Ra=500000 (d) Ra=1000000 while *Ha*=0 and Pr=0.71.

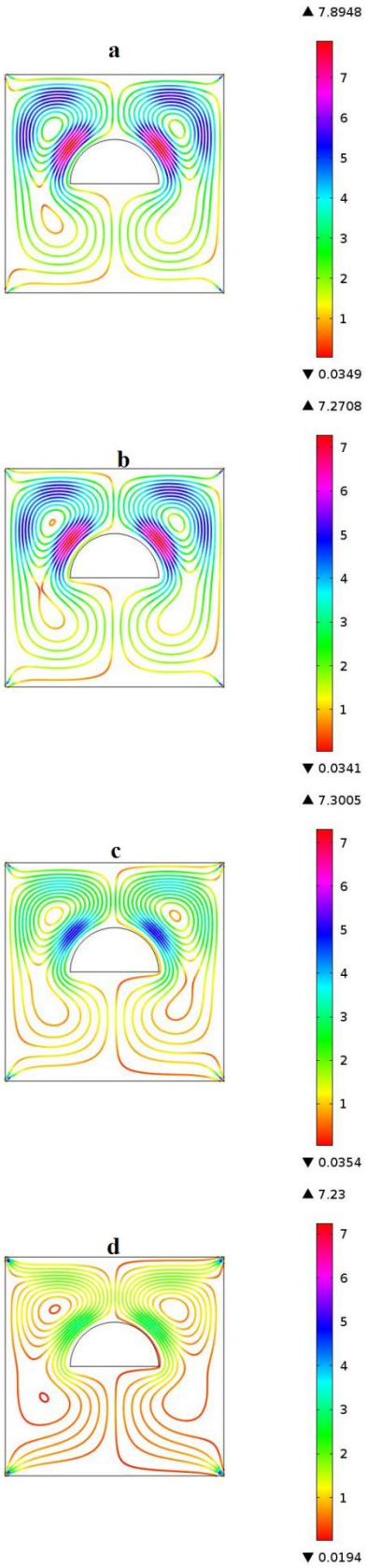

Fig. 5. Streamlines for (a) *Ha*=0; (b) *Ha*=20; (c) *Ha*=50, (a) *Ha*=100 while Pr=0.71 and *Ra*=10^5

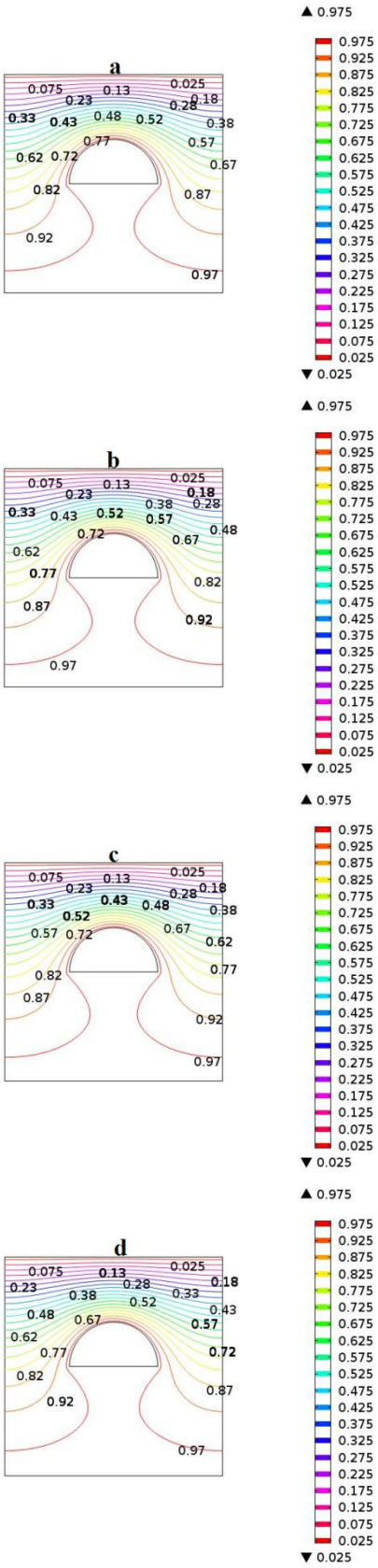

Fig. 6. Isotherms for (a) *Ha*=0; (b) *Ha*=20; (c) *Ha*=50, (a) *Ha*=100 while Pr=0.71 and *Ra*=10^5

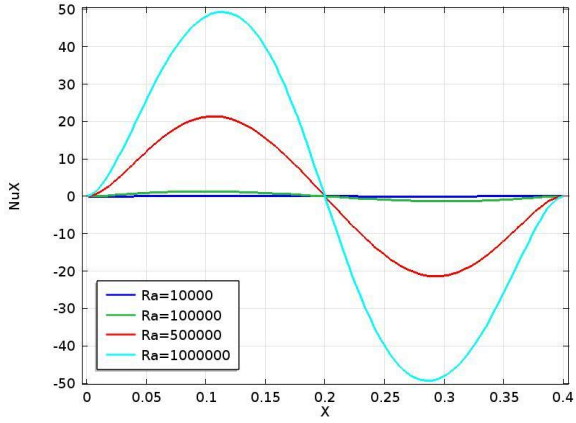

Fig. 7(a). Variation of local Nusselt number along the bottom wall for different Rayleigh number with Pr=0.71 and *Ha*=0.

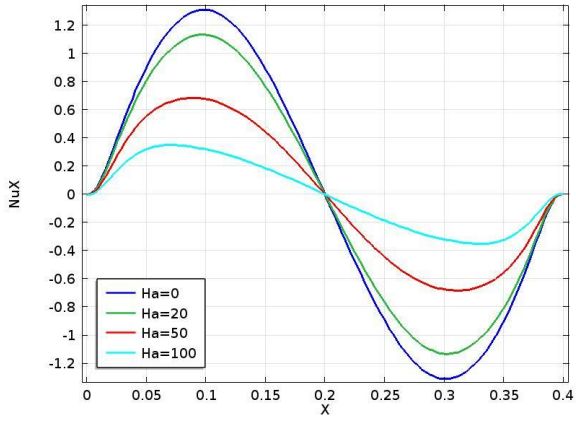

Fig. 7(b). Variation of local Nusselt number along the bottom wall for different Hartmann number with Pr=0.71 and R*a*=10^5.

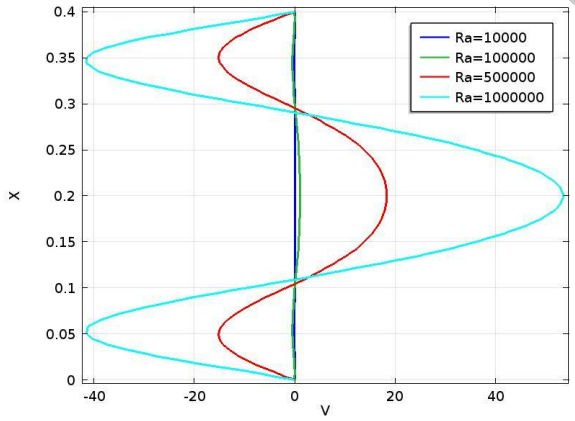

Fig. 8(a). Variation of velocity profiles along the bottom wall at different Rayleigh number with Pr=0.71 for *Ha*=0.

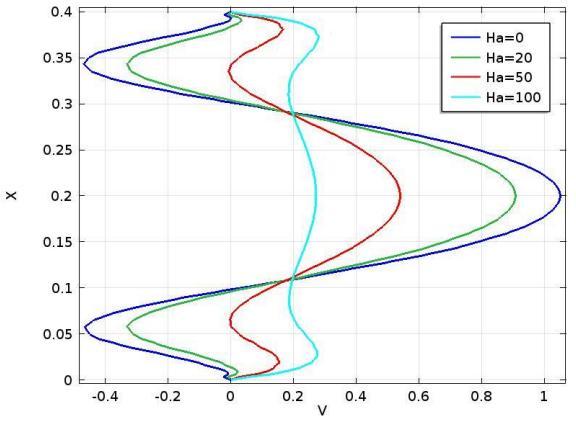

Fig. 8(b). Variation of velocity profiles along the bottom wall at different Hartmann number with Pr=0.71 and R*a*=10^5.

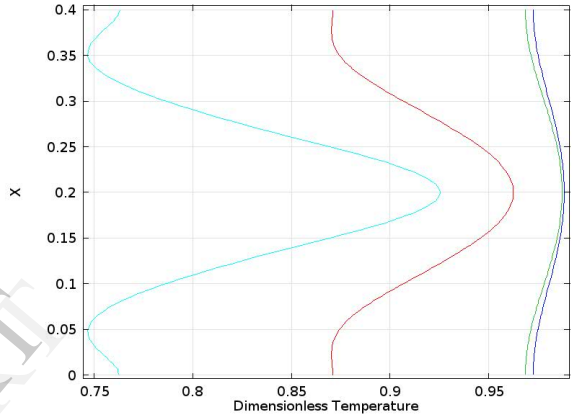

Fig. 9(a). Variation of temperature profiles along the bottom wall at different Rayleigh number with Pr=0.71 for *Ha*=0.

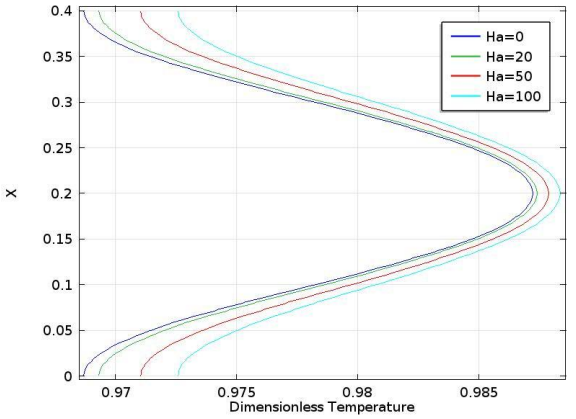

Fig. 9(b). Variation of temperature profiles along the bottom wall at different Hartmann number with Pr=0.71 and R*a*=10^5.

VI. CONCLUSION

Effect of Rayleigh and Hartmann numbers on the flow field in a square cavity with semicircular heated block along uniform magnetic field B_0 which is applied normal to the direction of the flow was studied numerically. The governing equations of mass, momentum and energy were solved using the Galerkin weighted residual method of finite element formulation. Various vortices entering into the flow field. From the present investigation the following conclusions may

be drawn as: with increase in the buoyancy force via increase in Rayleigh number, to decrease free convection, a stronger magnetic field is needed compared to the lower Rayleigh numbers.

REFERENCES

[1] Basak T., Roy S., Finite element analysis of natural convection flows in a square cavity with non-uniformly heated wall(s), Int. J. Eng. Sci., Vol. 43, Issues 8-9, pp. 668-680, 2005.

[2] Basak T., Roy S., Balakrishnan A.R., Effects of thermal boundary conditions on natural convection flows within a square cavity, Int. J. Heat Mass Transfer, Vol. 49, Issues 23-24, pp. 4525-4535, 2006.

[3] Öztop H.F. and Dagtekin I., Comparison of position of heated thin plate located in a cavity for natural convection, Int. Comm. Heat Mass Transfer, Vol. 31, No. 1, pp. 121-132, 2004.

[4] Öztop H.F. and Al-salem Khaled, Effects Of Joule Heating On MHD Natural Convection In Non-Isothermally Heated Enclosure, Journal of Thermal Science and Technology, Vol. 32, pp. 81-90, 2012.

[5] Mehmet C.E. and Elif B., Natural convection flow under a magnetic field in an inclined rectangular enclosure heated and cooled on adjacent walls, Fluid Dynamics Research, Vol. 38, pp. 564–590, 2006.

[6] Jani S., Mahmoodi M., Amini M., Magnetohydrodynamic Free Convection in a Square Cavity Heated from Below and Cooled from Other Walls, World Academy of Science, Engineering and Technology, International Journal of Mechanical, Industrial Science and Engineering Vol. 7, No.4, pp. 1-6, 2013.

[7] Saha G., Saha S., Mamun M.A.S., A finite element method for steady state natural convection in a square tilt open cavity, ARPN Journal of Engineering and Applied Sciences, Vol. 2, pp. 41-49, 2007.

[8] Reddy J.N., An Introduction to finite element method, Second Ed., McGraw-Hill Book Co. Singapore, 1993.